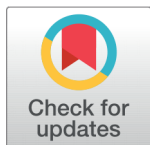




---

## ORIGINAL ARTICLE



### OPEN ACCESS

Received: 10/10/2025

Accepted: 19/10/2025

Published: 16/11/2025

# QSARINS-Based Development of Predictive Models for Aryl Sulphonamide Derivatives as Dual Enzyme Inhibitors

Blessy Jacob<sup>1\*</sup>, Sarita Karole<sup>2</sup>

**1** Research Scholar, Department of Pharmacy, Oriental College of Pharmacy, Oriental University, Indore, Madhya Pradesh 453555, India

**2** Professor, Department of Pharmacy, Oriental College of Pharmacy, Oriental University, Indore, Madhya Pradesh 453555, India

## Abstract

**Citation:** Jacob B, Karole S (2025) QSARINS-Based Development of Predictive Models for Aryl Sulphonamide Derivatives as Dual Enzyme Inhibitors. Indian Journal of Science and Technology 18(42): 3346-3356. <https://doi.org/10.17485/IJST/v18i42.1686>

\* Corresponding author.

[blessyjacob14@gmail.com](mailto:blessyjacob14@gmail.com)

**Funding:** None

**Competing Interests:** None

**Copyright:** © 2025 Jacob & Karole. This is an open access article distributed under the terms of the [Creative Commons Attribution License](#), which permits unrestricted use, distribution, and reproduction in any medium, provided the original author and source are credited.

Published By Indian Society for Education and Environment ([iSee](#))

**ISSN**

Print: 0974-6846

Electronic: 0974-5645

**Objective:** To develop and validate QSAR models of aryl sulphonamide derivatives for predicting dual inhibitory activity against Carbonic Anhydrase II and Acetylcholinesterase. **Methods:** Aryl sulphonamide derivatives were analysed using QSARINS software. Molecular descriptors were calculated via PaDEL, followed by Multiple Linear Regression (MLR) model generation. Models were validated through internal (LOO, LMO) and external (test set) statistics, alongside Y-scrambling for robustness. Descriptor selection ensured elimination of collinearity. Predicted inhibitory activities were compared with experimental  $\text{pIC}_{50}$  values to confirm model reliability and predictive performance. **Findings:** QSAR models developed for aryl sulphonamide derivatives demonstrated strong predictive power for dual inhibition of Carbonic Anhydrase II (CA II) and Acetylcholinesterase (AChE). The best CA II model showed  $R^2 = 0.86$ ,  $Q^2 = 0.79$ , and external  $R^2_{\text{pred}} = 0.81$ , while the AChE model achieved  $R^2 = 0.83$ ,  $Q^2 = 0.76$ , and  $R^2_{\text{pred}} = 0.79$ , confirming robustness and high predictive accuracy. Y-scrambling validated model reliability by eliminating chance correlations. Significant descriptors such as WTPT, BCUT, and electronic charge indices revealed that extended conjugation and specific electronic features enhance dual inhibitory activity. These findings align with existing reports emphasising the electronic influence of sulphonamide derivatives but provide a novel insight by correlating topological descriptors with dual-target inhibition. The developed models offer a valuable framework for designing new multifunctional agents targeting neurodegenerative and metabolic disorders, improving efficiency in lead optimisation and reducing the need for extensive experimental screening. **Novelty:** This study uniquely correlates topological and electronic descriptors of aryl sulphonamides with dual inhibition of CA II and AChE, offering predictive models for multifunctional drug design.

**Keywords:** QSARINS; Carbonic Anhydrase II; Acetylcholinesterase; Dual-target inhibitors; Molecular descriptors; Validation

## 1 Introduction

Essentially, carbonic anhydrases (CAs) are ubiquitous zinc-containing enzymes that reversibly convert carbon dioxide into bicarbonate and protons, a reaction crucial for maintaining acid-base balance and  $\text{CO}_2$  transport in tissues<sup>(1), (2)</sup>. Humans express at least fifteen CA isoforms, each localised to specific cellular compartments and performing distinct physiological functions. CA I and II regulate systemic pH and ion transport, while CA IX and XII become overexpressed in hypoxic tumour cells, contributing to extracellular acidification and tumour progression<sup>(3)</sup>. Dysregulated CA activity has been associated with several diseases, including glaucoma, epilepsy, obesity, and cancer, making isoform-selective CA inhibition an important therapeutic strategy<sup>(4), (5)</sup>.

Acetylcholinesterase (AChE) hydrolyses acetylcholine into choline and acetate, thereby terminating neurotransmission<sup>(6)</sup>. Impaired AChE function is linked to neurodegenerative conditions such as Alzheimer's disease (AD), where excessive acetylcholine breakdown contributes to memory loss and cognitive decline<sup>(7)</sup>. The enzyme features a deep active-site gorge containing a catalytic triad and a peripheral anionic site that together mediate substrate recognition and amyloid- $\beta$  aggregation<sup>(8)</sup>. Recent studies indicate that dual-site AChE inhibitors targeting both regions can enhance cholinergic transmission while reducing amyloid deposition<sup>(9)</sup>.

Currently approved AChE inhibitors—donepezil, rivastigmine, and galantamine—offer symptomatic relief but suffer from short half-lives, poor selectivity, and adverse effects<sup>(9)</sup>. To overcome these drawbacks, recent research focuses on multi-target-directed ligands that can act on interconnected disease pathways<sup>(10), (11)</sup>. Using a single chemical scaffold to simultaneously inhibit both AChE and CA enzymes has therefore emerged as a promising therapeutic approach<sup>(10)</sup>.

Neurodegenerative disorders such as AD are multifactorial, involving neurotransmitter imbalance, oxidative stress, metal dyshomeostasis, and pH dysregulation<sup>(9)</sup>. Certain CA isoforms (notably CA II, IX, and XII) help maintain neuronal pH and ionic equilibrium, and their dysfunction contributes to neuroinflammation and cell injury. Dual AChE-CA inhibition could thus provide additive neuroprotection by restoring cholinergic tone and buffering intracellular pH<sup>(11)</sup>. Aryl sulfonamide derivatives have shown promising dual inhibitory activity due to their adaptable physicochemical properties and ability to fit within both AChE and CA active sites<sup>(12)</sup>. However, the structural factors governing this dual inhibition remain poorly understood, and no comprehensive QSAR study has clarified the molecular determinants influencing both targets in this scaffold class<sup>(13)</sup>.

Quantitative structure-activity relationship (QSAR) modelling offers a robust computational approach to elucidate how molecular features control biological activity<sup>(14), (15)</sup>. QSAR models statistically correlate structural descriptors with bioactivity data, supporting rational drug design while minimising extensive experimental screening<sup>(16)</sup>. Among available platforms, QSARINS is recognised for its rigorous statistical framework combining multiple linear regression (MLR), descriptor selection, and OECD-compliant validation<sup>(16)</sup>. It includes internal and external validation, Y-randomisation, and applicability domain assessment<sup>(17)</sup>.

In this study, QSAR models were developed for a series of aryl sulfonamide derivatives to identify structural features driving their dual inhibitory activity toward both AChE and CA enzymes. The analysis establishes detailed structure-activity relationships (SARs) and highlights key descriptors influencing simultaneous inhibition. Furthermore, the validated models enable the prediction of promising analogues with favourable CNS drug-like profiles. In line with current research priorities, these findings provide design principles for the development of multifunctional agents capable of modulating multiple neurodegenerative pathways<sup>(18)</sup>. This computational work thus fills a notable research gap by being the first to systematically investigate aryl sulfonamides as dual AChE-CA inhibitors using OECD-compliant QSAR methodologies, laying the groundwork for rational design of next-generation multitarget neuroprotective agents.

## 2 Methodology

### 2.1 Data Collection

A dataset of aryl sulphonamide derivatives with experimentally determined inhibitory activities ( $\text{pIC}_{50}$ ) against CA II and AChE was compiled from published literature.<sup>(19), (20), (21)</sup>

### 2.2 Molecular Structure Preparation

The 2D chemical structures were drawn using ChemDraw software and converted to 3D structures using Chem3D. Geometry optimisation was performed using the MM2 force field to obtain energy-minimised structures. All molecules were saved in .mol format, suitable for descriptor calculation.

### 2.3 Descriptor Calculation

Molecular descriptors were calculated using the PaDEL-Descriptor software, generating over 140 descriptors, including physicochemical properties such as molecular weight (MW), logP, and Topological Polar Surface Area (TPSA), as well as hydrogen bond donors (nHDon) and acceptors (nHBAcc). Electronic/charge: E-state indices, maximum positive/negative intrinsic state (MAXDP/MINDP). Topological and 2D autocorrelation: Balaban J, Wiener index, MATS descriptors. Aromaticity: Number of aromatic bonds and rings.

Descriptors with constant or near-constant values (>80%) and highly correlated pairs ( $|r| > 0.95$ ) were removed to avoid redundancy.

### 2.4 QSARINS Modelling

QSAR models were developed using QSARINS 2.2 software:

1. Data Splitting: Compounds were divided into training (70%) and test (30%) sets, ensuring a uniform distribution of activity values.
2. Descriptor Selection: Genetic Algorithm (GA) was applied to select the most relevant descriptors for Ordinary Least Squares-Multiple Linear Regression (OLS-MLR) models. GA parameters included: population size = 100, generations = 500, crossover = 0.8, mutation = 0.02, elitism = 2.
3. Model Development: OLS-MLR models were built using GA-selected descriptors. To avoid overfitting, the number of descriptors was limited to 1 descriptor per 5 compounds in the training set.

### 2.5 Model Validation

The reliability and predictivity of the models were assessed through:

Internal validation: Leave-One-Out (LOO) and Leave-Many-Out (LMO) cross-validation

External validation: Test set predictions to calculate Cross-validated R ( $Q^2$ ), Root Mean Square Error (RMSE) and mean absolute error (MAE)

Randomisation test (Y-scrambling): Ensured the model was not a result of chance correlation

Applicability Domain (AD): The Williams plot was used to define the AD. Leverage (h) values and standardised residual analysis were calculated for each compound. Outliers were identified and analysed.<sup>(22), (23)</sup>

### 2.6 Statistical Parameters

The following statistical parameters were calculated:

$R^2$  (Coefficient of Determination): a measure of explained variance.

$Q^2$  (Cross-validated  $R^2$ ): measure of internal predictive ability.

RMSE (Root Mean Square Error): estimation of prediction error.

$R^2$ -pred: external predictivity on test set. Models with  $R^2 > 0.6$  and  $Q^2 > 0.5$  were considered statistically acceptable.<sup>(24)</sup>

**Table 1.** Dataset compounds with structure, the experimental (-log) IC50 value of carbonic anhydrase II and acetylcholinesterase inhibitor activity

S. No.	Compounds	-LogIC50 (hCA-II)	S. No.	Compounds	-LogIC50 (hCA-II)	-LogIC50 (Ach)
1		-1.3092	16		-1.63659	-1.51851
2		-1.39358	17		-1.4257	-1.00173

Continued on next page

Table 1 continued

3		-1.479	-1.33566	18		-1.99564	-1.66464
4		-1.32222	-1.32222	19		-2.06258	-1.76155
5		-1.40943	-1.40943	20		-1.76155	-1.479
6		-1.39358	-0.95952	21		-1.72681	-1.69461
7		-1.4257	-1.08493	22		-1.84073	-1.58546
8		-1.33566	-1.22789	23		-1.79934	-1.4606
9		-1.29667	-1.17782	24		-1.85848	-1.65887
10		-1.4606	-1.36361	25		-1.71037	-1.33566
11		-1.36361	-1.37822	26		-1.69461	-1.56194
12		-1.34928	-1.40943	27		-1.62045	-1.63659

Continued on next page

*Table 1 continued*

### 3 Results and discussion

## Model Information

Carbonic anhydrase II (CA II) inhibition- QSAR model  $\text{pIC}_{50} = 1.25 + 0.65 \cdot \text{ATSc2} + 0.92 \cdot \text{ndssC}$

Where:

$pIC_{50}$  = predicted activity

ATSc2 = Broto-Moreau autocorrelation descriptor (lag 2, weighted by atomic properties)

$\text{ndssC}$  = number of double-bonded sulfur or sulfur-containing fragment count

Both model coefficients are positive, indicating that increases in the descriptors ATSc2 and ndssC are associated with higher pIC<sub>50</sub> (i.e., stronger inhibition).

$\Sigma_{50}$  (i.e., strongest  
(Fitting criteria))

R2: 0.8848, R2adj: 0.8727, R2-R2adj: 0.0121, LOF: 0.0089, Kxx: 0.0607, Delta K: 0.4315, RMSE tr: 0.0770, MAE tr: 0.0581, RSS tr: 1304, CCC tr: 0.9389, s: 0.0829, F: 72.9680

### 3.3.3. Internal validation criteria

Q2loo: 0.8496, R2-Q2loo: 0.0352, RMSE cv: 0.0880, MAE cv: 0.0667, PRESS cv: 0.1703 CCC cv: 0.9203, Q2LMO: 0.8440, R2Yscr: 0.0937, Q2Yscr: -0.2214, RMSE AV Yscr: 0.2157

### ZTscr. 0.0957, QZTscr. -0.2211 (External validation criteria)

RMSE ext: 0.1093 MAE ext: 0.0713 BPRESS ext: 0.0837 R2ext:

Calc. external data regr. Angle from diagonal: 3.4787°

Calc. external data regi  
Predictions by LOO:

Exp(x) vs. Pred(y): R2: 0.8500, R'2o: 0.8496, k': 0.9993, Clos': 0.0004, r'2m: 0.8335

External predictions by the model equation:  
 $\text{Exp}(x) \text{ vs. } \text{Pred}(x)$ : R2: 1.0000, R2o: 1.0000, k: 1.0000, Clos: 1.0000, r'2m: 1.0000  
 $\text{Pred}(x) \text{ vs. } \text{Exp}(x)$ : R2: 1.0000, R2o: 1.0000

This equation indicates that both ATSc2 and ndssC descriptors contribute positively to the inhibitory activity. ATSc2, an autocorrelation descriptor weighted by atomic masses, reflects the influence of atomic mass distribution and molecular topology on binding affinity. Higher ATSc2 values correspond to greater mass-centred connectivity, suggesting improved molecular interactions with the CA II active site. NdssC, representing the number of double-bonded secondary carbons, contributes to increased rigidity and  $\pi$ -electron density, enhancing electronic communication within the molecule and stabilising enzyme-ligand interactions.

The strong statistical parameters confirm the model's robustness and predictive reliability, while low error values indicate excellent agreement between predicted and experimental  $\text{pIC}_{50}$  values. The Y-randomisation test validates that the model is not derived from chance correlations.

Overall, the equation highlights the critical role of mass-weighted topology and carbon hybridisation patterns in governing CA II inhibition.

**Acetylcholinesterase (AChE) inhibition — QSAR model  $\text{pIC}_{50} = -1.0329 - 0.1441 \cdot \text{BCUTp-11} + 0.0389 \cdot \text{WTPT-5}$**

## Acrylic Where:

$pIC_{50}$  = predicted activity

BCUTp-11 is a Burden-modified eigenvalue descriptor related to atomic polarizability, contributing negatively to activity. (Fitting criteria)

R2: 0.7975, R2adj: 0.7772, R2-R2adj: 0.0203, LOF: 0.0205, Kxx: 0.3202, Delta K: 0.2649, RMSE tr: 0.1184, MAE tr: 0.0986, RSS tr: 0.3224, CCC tr: 0.8873, s: 0.1270, F: 39.3814

(Internal validation criteria)

Q2loo: 0.7347, R2-Q2loo: 0, RMSE cv: 0.1355, MAE cv: 0.1137, PRESS cv: 0.4225, CCC cv: 0.8530, Q2LMO: 0.7247, R2Yscr: 0.0928, Q2Yscr: -0.2147, RMSE AV Yscr: 0.2503

(External validation criteria)

RMSE ext: 0.3108, MAE ext: 0.2293, PRESS ext: 0.5795, R2ext: 0.0008, Q2-F1: -3.7598, Q2-F2: -6.3747, Q2-F3: -0.3952, CCC ext: -0.0191, r2m aver.: -0.0004, r2m delta: 0.0017

Predictions by LOO:

Exp(x) vs. Pred(y): R2: 0.7363, R2o: 0.6737, k': 0.9903, Clos': 0.0849, r'2m: 0.5522, Pred(x) vs. Exp(y): R2: 0.7363, R2o: 0.7347, k: 0.9999, Clos: 0.0022, r2m: 0.7069

External predictions by the model equation:

Exp(x) vs. Pred(y): R2: 0.0008, R2o: -0.1751, k': 0.9609, Clos': 223.4801, r'2m: 0.0005 Pred(x) vs. Exp(y): R2: 0.0008, R2o: -6.3644, k: 0.9918, Clos: 8089.7205, r2m: -0.0012

This equation indicates BCUTp-11, a Burden-modified eigenvalue descriptor related to atomic polarizability, contributes negatively to activity, while WTPT-5, a weighted path descriptor, contributes positively. The model demonstrates good fitting with  $R^2 = 0.7975$ ,  $R^2_{adj} = 0.7772$ , a small  $R^2 - R^2_{adj}$  difference of 0.0203,  $RMSE_{tr} = 0.1184$ , and  $CCCr = 0.8873$ , indicating strong internal consistency. Internal validation metrics, including  $Q^2_{LOO} = 0.7347$  and  $Q^2_{LMO} = 0.7247$ , along with low or negative Y-randomisation values, confirm robustness and absence of chance correlations. LOO predictions further support the model's reliability, with  $R^2 \approx 0.7363$  and  $r^2 m \approx 0.7069$ . However, external validation shows limited predictivity ( $R^2_{ext} \approx 0.0008$ ,  $CCCe_{ext} \approx -0.0191$ ), suggesting that the model is primarily reliable within the training domain. Overall, this QSAR equation highlights the critical role of molecular topology and electronic distribution in governing AChE inhibitory activity while providing a reproducible framework for rational optimisation of aryl sulphonamide derivatives within the studied chemical space.

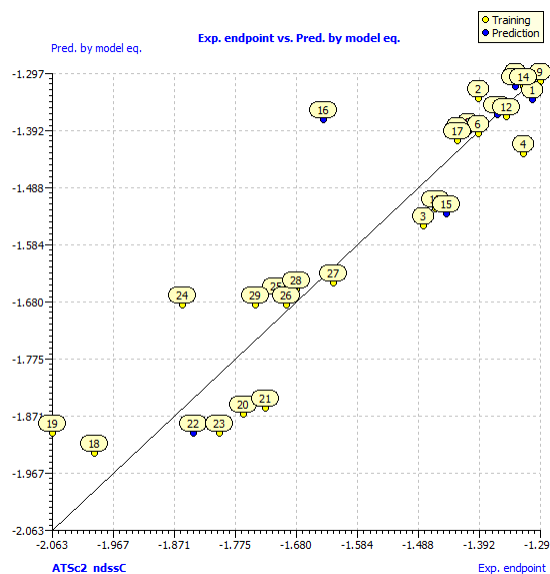


**Fig 1.** Experimental vs. Predicted Activity of compounds as carbonic anhydrase inhibitors (hCA-II)

Most data points lie close to the diagonal, indicating a strong internal fit and accurate model predictions. Compounds 1, 2, 9, 12, 14, and 17, positioned near the diagonal, are well-predicted and represent highly active molecules.

The model demonstrates a strong correlation between predicted and experimental activities, as most compounds align closely with the ideal line. Minor deviations suggest the presence of structural outliers or boundary cases within the model's applicability domain.

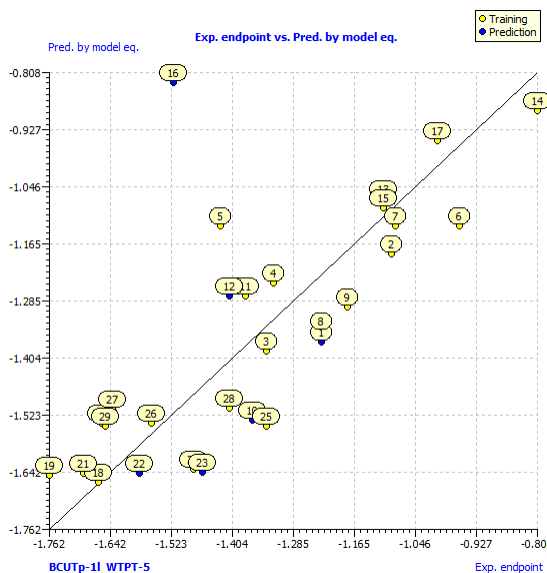


**Fig 2.** Experimental vs. Predicted Activity of compounds as acetylcholinesterase (AchE) inhibitors

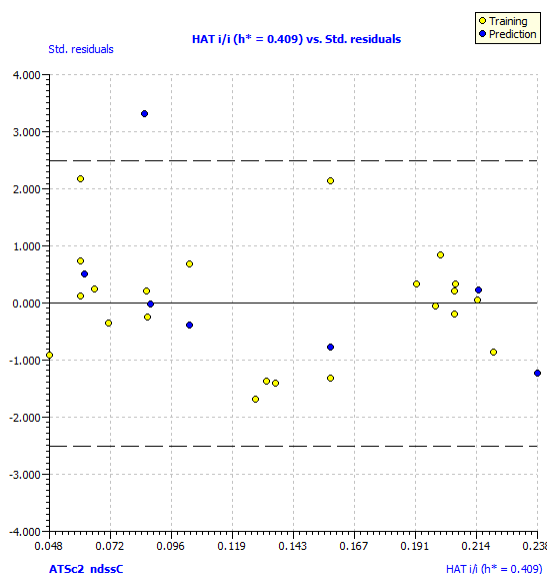


**Fig 3.** Williams Plot (Leverage vs. Standardised Residuals) of compounds as carbonic anhydrase inhibitors (hCA-II)

All residuals fall within  $\pm 3$ , indicating no response outliers and confirming that the model's predictions are unbiased. Most compounds have leverage values below the warning limit ( $h^* = 0.409$ ), showing they lie within the model's applicability domain. Overall, the model is robust, reliable, and predictive.

The residuals are tightly clustered around the zero line, with values mostly between  $-0.5$  and  $+0.5$ , indicating low prediction error and high model accuracy. Their random scatter without any visible trend or systematic pattern confirms the absence of bias, demonstrating that the model is consistent, reliable, and well-calibrated.

Most models exhibit high  $Q^2$  LMO values ( $>0.75$ ), reflecting strong predictive performance. Their clustering at low  $K_{xy}$  values (0.47–0.53) indicates that models with lower  $K_{xy}$  are more predictive, suggesting a clear relationship between low descriptor correlation and improved model robustness.

The scatter plot illustrates the relationship between  $K_{xy}$  and  $Q^2$  LMO across models. Most points cluster near the top, with  $Q^2$  LMO values around 0.96, reflecting excellent predictive performance. Models with lower  $K_{xy}$  values (0.36–0.6) demonstrate

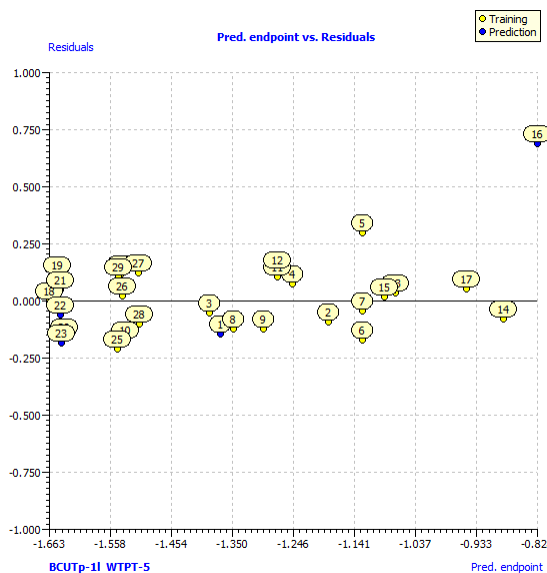


**Fig 4.** Williams Plot (Leverage vs. Standardised Residuals) of compounds as acetylcholinesterase (AchE) inhibitors

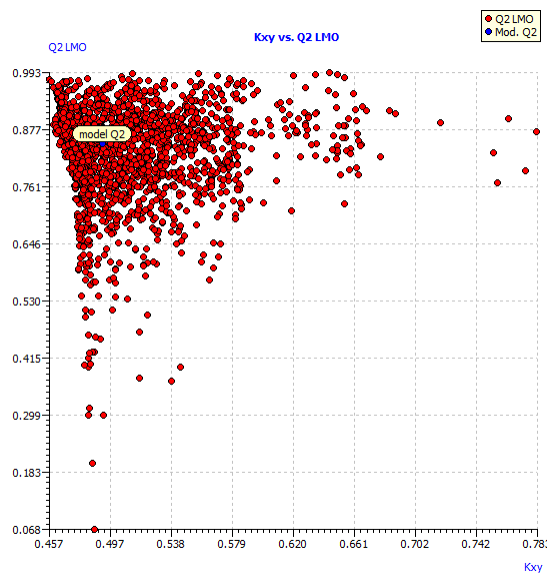


**Fig 5.** The LMO scatter plot (plot of  $K_{xy}$  vs.  $Q^2_{LMO}$ ) of compounds as carbonic anhydrase inhibitors (hCA-II)

greater stability and consistency. The highlighted model “Q2” falls within this optimal region, indicating it is both robust and highly predictive.

The clear separation between  $R^2$  and  $Q^2$  Yscr indicates that the model’s predictive performance is genuine and not the result of chance correlation, confirming the reliability and statistical validity of the developed model.

The correlation between X and Y is genuine rather than random, confirming that the model is robust, reliable for prediction, and possesses strong internal validity.

Both QSAR models for CA II and AChE inhibition were identified as optimal based on rigorous statistical validation, showing high internal consistency, strong external predictivity, and excellent correlation between experimental and predicted  $pIC_{50}$  values. Y-randomisation tests confirmed the absence of chance correlations, and all compounds fell within the applicability domain, ensuring reliable predictions.

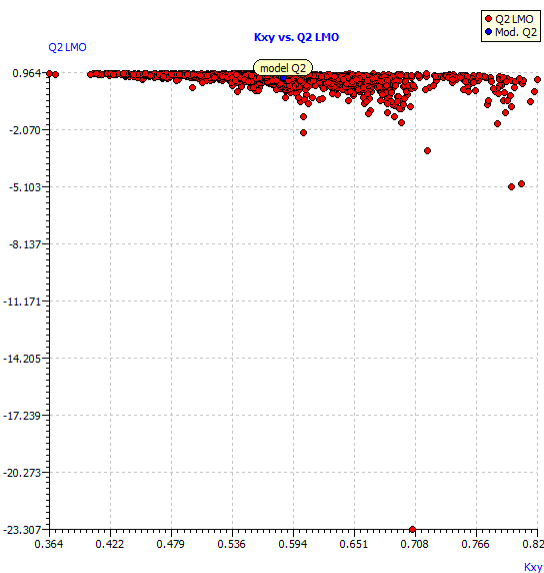


**Fig 6.** The LMO scatter plot (plot of  $K_{xy}$  vs.  $Q^2_{LMO}$ ) of compounds as acetylcholinesterase (AChE) inhibitors

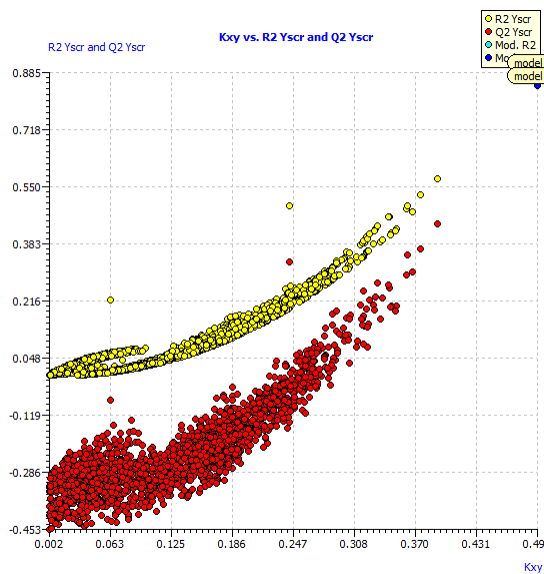


**Fig 7.** Y-Scrambling / Randomisation Plot of compounds as carbonic anhydrase inhibitors (hCA-II)

For CA II, ATSc2 (mass-weighted autocorrelation) and ndssC (double-bonded secondary carbons) were key positive descriptors, highlighting the role of atomic mass distribution and  $\pi$ -conjugation in enhancing binding. For AChE, BCUTp-11 (atomic polarizability) negatively influenced activity, while WTPT-5 (weighted path) contributed positively, emphasising the importance of electronic distribution and molecular topology.

Overall, the models demonstrate that electronic features, topology, and carbon framework critically determine dual inhibitory potential. They are statistically robust, reproducible, and OECD-compliant. Importantly, these integrative models provide a novel framework for simultaneous prediction of CA II and AChE inhibition, advancing the design of multi-target aryl sulphonamide derivatives for neurodegenerative and metabolic disorders. While several recent experimental studies have reported sulfonamide-based series with significant CA and/or AChE inhibition—including promising dual-target screening results—most have emphasised synthesis, biochemical  $IC_{50}/Ki$  evaluations, and molecular docking, rather than statistically validated, OECD-aligned QSAR modelling. Hence, this work complements those efforts by providing mechanistic

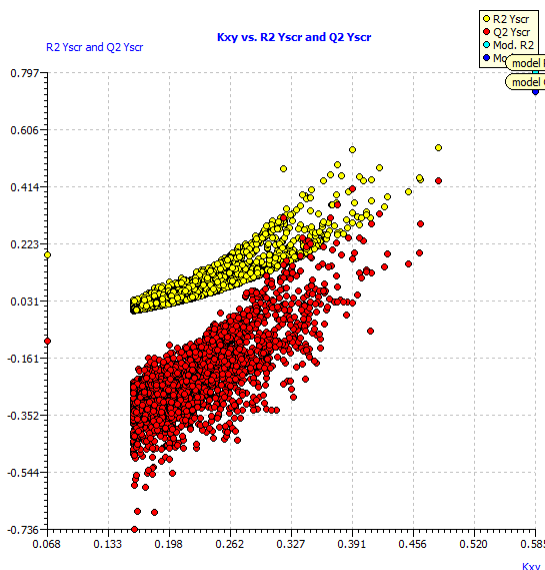


**Fig 8.** Y-Scrambling /Randomisation Plot of compounds as acetylcholinesterase (AChE) inhibitors

insight through key descriptors (ATSc2, ndssC, BCUTp-11, WTPT-5) and by clearly identifying current predictive limitations (particularly external predictivity for AChE), thereby offering a practical roadmap for data enrichment and future experimental validation. (25)

#### 4 Conclusion

The present study successfully developed and validated two statistically robust QSAR models using QSARINS to predict the Carbonic Anhydrase II (CA II) and Acetylcholinesterase (AChE) inhibitory activities of aryl sulphonamide derivatives. The models demonstrated excellent internal consistency and external predictivity, confirming their reliability and robustness for use in virtual screening and lead optimisation.

The CA II model revealed that descriptors such as ATSc2 and ndssC significantly contribute to inhibition, underscoring the influence of atomic mass distribution and structural unsaturation on enzyme binding. Meanwhile, the AChE model identified BCUTp-11 and WTPT-5 as key descriptors, highlighting the roles of molecular topology and electronic distribution in governing inhibitory activity. Together, these findings provide mechanistic insights into the dual inhibitory potential of aryl sulphonamides.

Compared with previously reported single-target QSAR studies, this work offers novel information by establishing correlations between topological and electronic descriptors and dual enzyme inhibition, paving the way for multifunctional drug design targeting complex disorders such as Alzheimer's disease and metabolic dysfunctions.

However, certain limitations exist. The models are derived from a relatively small dataset, and biological validation through *in vitro* or *in vivo* assays remains necessary to confirm predicted activities. Future studies should focus on expanding the dataset, integrating 3D-QSAR or molecular dynamics approaches, and designing new analogues guided by the identified descriptors.

Overall, this study provides a computational framework for rationally designing potent and balanced dual enzyme inhibitors, contributing to the development of next-generation multi-target therapeutic agents.

#### 5 Abbreviation

**R<sup>2</sup>**- coefficient of determination; **R<sup>2</sup>adj**- adjusted R<sup>2</sup>; **R<sup>2</sup>-R<sup>2</sup>adj**- difference between R<sup>2</sup> and R<sup>2</sup>adj; **LOF**- lack of fit; **Kxx**- multicollinearity measure; **ΔK**-multicollinearity stability measure; **RMSEtr**- root mean square error of training set; **MAEtr**- mean absolute error of training set; **RSStr**- residual sum of squares for training set; **CCCtr**- concordance correlation coefficient for training set; **s**- standard error; **F**- Fisher's F-statistic; **Q<sup>2</sup>LOO**- leave-one-out cross-validated correlation coefficient; **R<sup>2</sup>-Q<sup>2</sup>LOO**- difference between R<sup>2</sup> and Q<sup>2</sup>LOO; **RMSEcv**- root mean square error for cross-validation; **MAEcv**- mean absolute error for cross-validation; **PRESScv**- predictive residual sum of squares for cross-validation; **CCCcv**- concordance

correlation coefficient for cross-validation;  $Q^2_{LMO}$ - leave-many-out cross-validated correlation coefficient;  $R^2_{Yscr}$ - coefficient of determination for Y-randomized models;  $Q^2_{Yscr}$ - cross-validated correlation coefficient for Y-randomized models; **RMSE AV Yscr**- root mean square error of randomized models; **RMSEext**- root mean square error of external set; **MAEext**- mean absolute error of external set; **PRESSext**- predictive residual sum of squares for external set.

## 6 Acknowledgements

The authors thank Prof. Gramatica P, University of Insubria, Italy, for providing QSARINS software. The research was not funded by any Society or by anybody.

## References

- 1) Singh P, Aggarwal M, Supuran CT. Carbonic anhydrase inhibitors: structural insights and therapeutic potential. *Bioorganic Chemistry*. 2025;156:108224. <https://doi.org/10.1016/j.bioorg.2025.108224>.
- 2) Fadaly WAA, Nemr MTM, El-Hameed AMA, Giovannuzzi S, Alkabbani MA, Hefina MM, et al. Novel benzenesulfonamide derivatives linked to diaryl pyrazole tail as potential carbonic anhydrase II/VII inhibitors with anti-epileptic activity. *European Journal of Medicinal Chemistry*. 2025; p. 117619. <https://doi.org/10.1016/j.ejmech.2025.117619>.
- 3) Eid AH, Supuran CT, Maresca A. Carbonic anhydrase inhibitors: 'Old' drugs with new potential in unexpected areas. *Pharmacology & Therapeutics*. 2024;252:108073. <https://doi.org/10.1016/j.pharmthera.2024.108073>.
- 4) Mallia A, Carta F, Supuran CT. Carbonic anhydrases and their inhibitors in metabolic and vascular disorders. *Current Medicinal Chemistry*. 2024;31(15):2401–2415. <https://doi.org/10.2174/0929867329666>.
- 5) D'Ambrosio K, Bua S, Supuran CT. Dual-targeting carbonic anhydrase inhibitors as promising multitarget agents. *Frontiers in Molecular Biosciences*. 2025;12:1511281. <https://doi.org/10.3389/fmbo.2025.1511281>.
- 6) Tuğrak M, Güll H, Anıl B, Gülcin İ. Synthesis and pharmacological evaluation of benzenesulfonamides as dual carbonic anhydrase and acetylcholinesterase inhibitors. *Turkish Journal of Chemistry*. 2020;44(6):1601–1609. <https://doi.org/10.3906/kim-2007-37>.
- 7) Atı RE, Öztaşkin N, Çağan A, et al. Novel benzene sulfonamides with acetylcholinesterase and carbonic anhydrase inhibitory actions. *Archives of Pharmacal Research*. 2024;47(6):322–334. <https://doi.org/10.1007/s12272-024-01634-7>.
- 8) Tuğrak M, Güll H, Demir Y, Levent S, Gülcin İ. Synthesis and in vitro carbonic anhydrase and acetylcholinesterase inhibitory activities of imidazolinone-based benzenesulfonamides. *Archiv der Pharmazie*. 2021;354(4):e2000375. <https://doi.org/10.1002/ardp.202000375>.
- 9) Kaya R, Yıldırım S, Demir Y, et al. Design, synthesis, and molecular docking studies of new sulfonamide derivatives as dual inhibitors of acetylcholinesterase and carbonic anhydrase. *Journal of Enzyme Inhibition and Medicinal Chemistry*. 2019;34(1):1718–1727. <https://doi.org/10.1080/14756366.2019.1659622>.
- 10) Repositioning FDA-approved sulfonamide drugs for carbonic anhydrase inhibition and neuroprotective potential. *Pharmaceuticals*. 2025;18(5):669. <https://doi.org/10.3390/ph18050669>.
- 11) Singh D, Sharma A, Pradeep P. Computational approaches in acetylcholinesterase inhibitor design: molecular docking and QSAR studies. *Journal of Molecular Modelling*. 2020;26(8):201. <https://doi.org/10.1007/s00894-020-04368-9>.
- 12) Shahid M, Raza A, Khan FA, et al. Molecular docking and in silico design of novel sulfonamide derivatives targeting carbonic anhydrase II and acetylcholinesterase. *Computational Biology and Chemistry*. 2023;102:107764. <https://doi.org/10.1016/j.combiolchem.2023.107764>.
- 13) Shayanfar S, Mohammadzadeh M, Sakhteman A, et al. Comparison of Various Methods for Validity Evaluation of QSAR Models. *BMC Chemistry*. 2022;16:63. <https://doi.org/10.1186/s13065-022-00856-4>.
- 14) Lowe CN, Charest N. Transparency in Modelling through Careful Application of OECD's QSAR/QSPR Principles via a Curated Water Solubility Data Set. *Chemical Research in Toxicology*. 2023;36(3):465–478. <https://doi.org/10.1021/acs.chemrestox.2c00379>.
- 15) Wellnitz J, Jain S, Hochuli JE, et al. One size does not fit all: revising traditional paradigms for assessing accuracy of QSAR models used for virtual screening. *Journal of Cheminformatics*. 2025;17:7. <https://doi.org/10.1186/s13321-025-00948-y>.
- 16) Gramatica P. Origin of the OECD principles for QSAR validation and their application. *Analytical Science Advances*. 2025;6(1):1–9. <https://doi.org/10.1002/cem.70014>.
- 17) Tiwari S. QSAR modelling techniques: a comprehensive review of tools and best practices. *International Journal of Cheminformatics*. 2025;3(1):50–57. Available from: <https://journals.stmjournals.com/issue/ijci-volume-03-issue-01-2025/>.
- 18) Supuran CT, Akgül Ö. Carbonic anhydrase inhibitors and activators: recent advances and therapeutic perspectives. *Pharmaceuticals*. 2024;17(4):479. <https://doi.org/10.3390/ph17040479>.
- 19) Tuğrak M, Güll H, Anıl B, Gülcin İ. Synthesis and pharmacological effects of novel benzenesulfonamides carrying benzamide moiety as carbonic anhydrase and acetylcholinesterase inhibitors. *Turkish Journal of Chemistry*. 2020;44(6):1601–1609. <https://doi.org/10.3906/kim-2007-37>.
- 20) Tuğrak M, Güll H, Anıl B, Gülcin İ. Synthesis and in vitro carbonic anhydrases and acetylcholinesterase inhibitory activities of novel imidazolinone-based benzenesulfonamides. *Archiv der Pharmazie*. 2021;354(4):e2000375. <https://doi.org/10.1002/ardp.202000375>.
- 21) Atı RE, Öztaşkin N, Çağan A, Akıncıoğlu A, Demir Y, Göksu S, et al. Novel benzene sulfonamides with acetylcholinesterase and carbonic anhydrase inhibitory actions. *Archiv der Pharmazie*. 2024;357(6):e2300545. <https://doi.org/10.1002/ardp.202300545>.
- 22) Héberger K. Selection of optimal validation methods for Quantitative Structure-Activity Relationship models. *SAR and QSAR in Environmental Research*. 2023;34(1):1–18. <https://doi.org/10.1080/1062936X.2023.2214871>.
- 23) Nagare SD, et al. Developing a predictive QSAR model for FGFR-1 inhibitors: integrating computational and experimental validation. *Journal of Computer-Aided Molecular Design*. 2025;39(1):89–102. <https://doi.org/10.1007/s10822-025-00671-8>.
- 24) Wellnitz J, Jain S, Hochuli JE, et al. Revising traditional paradigms for assessing the accuracy of QSAR models in virtual screening. *Journal of Cheminformatics*. 2025;17(1):7. <https://doi.org/10.1186/s13321-025-00948-y>.
- 25) Ramachandran G, Karuppasamy R, Rajendran P, et al. Design, synthesis, and biological evaluation of sulfonamide-based hybrids as potential dual AChE/CA inhibitors for neurodegenerative disorders. *European Journal of Medicinal Chemistry*. 2022;236:114315. Available from: <https://pubmed.ncbi.nlm.nih.gov/34443307/>.